AUTHOR(S): DROUBI, M.G., FAISAL, N.H., STUART, A., MOWAT, J., NOBEL, C. and EL-SHAIB, M.N.

TITLE: Acoustic emission testing of composite-to-metal and metal-to-metal adhesive bond strengths.

YEAR: 2016

Publisher citation: DROUBI, M.G., FAISAL, N.H., STUART, A., MOWAT, J., NOBEL, C. and EL-SHAIB, M.N. 2016. Acoustic emission testing of composite-to-metal and metal-to-metal adhesive bond strengths. In Proceedings of the 32nd European conference on acoustic emission testing [EWGAE 2016], 7-9 September 2016, Prague, Czech Republic. Bad Breisig: NDT.net [online], pages 95-104. Available from: http://www.ndt.net/article/ewgae2016/papers/95_paper.pdf

OpenAIR citation: DROUBI, M.G., FAISAL, N.H., STUART, A., MOWAT, J., NOBEL, C. and EL-SHAIB, M.N. 2016. Acoustic emission testing of composite-to-metal and metal-to-metal adhesive bond strengths. In Proceedings of the 32nd European conference on acoustic emission testing [EWGAE 2016], 7-9 September 2016, Prague, Czech Republic. Bad Breisig: NDT.net, pages 95-104. Held on OpenAIR [online]. Available from: http://openair.rgu.ac.uk.

Czech Society for Nondestructive Testing
32nd European Conference on Acoustic Emission Testing
Prague, Czech Republic, September 07-09, 2016

ACOUSTIC EMISSION TESTING OF COMPOSITE-TO-METAL AND METAL-TO-METAL ADHESIVE BOND STRENGTHS

Mohamad G. DROUBI[1], Nadimul H. FAISAL[1], Alan STUART[1], John MOWAT[1], Craig NOBEL[1], Mohamed N. EL-SHAIB[2]

[1] School of Engineering, Robert Gordon University, Garthdee Road, Aberdeen, AB10 7GJ, UK
Phone: +441224262336; e-mail: m.g.droubi@rgu.ac.uk n.h.faisal@rgu.ac.uk
[2]Marine Engineering Department, Arab Academy for Science, Technology and Maritime Transportation, Alexandria, Egypt

Abstract

Composite sandwich structures consisting of two layers with an adhesive contacting interface are of importance in a number of industrial applications such as aerospace, marine and automotive. This research therefore aims to characterise the failure behaviour of adhesively bonded specimen (e.g. carbon fibre reinforced composite-tometal adhesive bonded substrates) and failure modes namely Mode I: double cantilever beam (DCB) and Mode II: three-point end notch flexures (3-ENF) using the acoustic emission (AE) monitoring technique. AE may aid in the understanding of the mechanics behind the specified failure modes of adhesively joined composite structures. In order to control the adhesively bonded area, a dry anti-stick film was applied to the mating surfaces, which can simulate a bonding quality. Twelve adhesively bonded specimens, for each failure mode, were prepared using two types of adhesive bond materials (acrylic-based ductile bond and cyanoacrylate-based brittle bond) with three variations of adhesive bond quality. Prior to mechanical testing, the adhesive bonded specimens were examined using AE to obtain understanding of signal transmission within the structure.

It was possible for the maximum AE amplitude method to select the AE events of mechanical significance (e.g. adhesive failure, substrate deformation) for further identification through thorough analysis. From this maximum AE amplitude method, it was possible to distinguish between the different AE sources of mechanical significance. However, it was proved difficult to propose a definitive AE trait for the mechanical phenomena occurring within specific AE event signals, for all adhesive types, bond qualities, and substrate configurations; therefore all specimen combinations. There was a notable shift in spectral energy proportion as the AE source of mechanical significance varied along the specimen length for particular specimen combinations. However, it was difficult to confirm this distinctive trait for all specimen combinations due to difficulty in confirming the location and exact mechanical source. However, the proposed measurement technique can be useful to assess the overall structural health of a bonded system (e.g. pipe-in-pipe) and may allow identification of defects that can significantly reduce the strength and reliability of material, consequently increasing the risk of component failure.

Keywords: Acoustic Emission (AE), failure mode, adhesive bond strength.

1. Introduction

The joining of two or more materials is necessary throughout many applications as it allows physical properties from both or all materials to be utilised. There are different methods to join two or more substrate (e.g. mechanical fastening, thermal joining and adhesive bonding). The application of adhesive bonding is used in aerospace applications, automotive engineering and marine structures as it provides weight saving, elimination of holes, electrical insulation and improved stiffness. Understanding the potential modes of failure for adhesively bonded structure is a key aspect in evaluating their structural integrity. Therefore, this paper aims to develop the technique of Acoustic Emission (AE) in order to monitor the mechanical properties and failure modes of various material combinations that are bonded together using adhesive.

Bak *et al* [1], have investigated the generation of AE from adhesively bonded lap joints with particular focus towards aerospace structures. They determined the occurrence of substrate failure through photographic evidence and also declared the misconception that the lower the bond thickness, the greater the bond strength. Furthering research using nano-tubing reinforced bonds on single lap joints with both composite and steel substrates with implementation of AE, in pursuit of enhancing adhesive strength, was carried out by Lim *et al* [2]. They observed a steady increase of AE counts from initial loading to failure for all types of failure (adhesive, substrate or combined), however, it is clear that there is a higher cumulative of signals close to joint failure produced when subjected to substrate failure, with the least generated from an adhesive failure.

AE signals generated through varying bond qualities of single lap joints using voids or disbands (induced weak bond between adhesive and substrate) was investigated by NayebHashemi *et al* [3] using steel substrates. They observed that AE signals regarding the artificial voids or disbond's created short, high energy releases at failure in comparison with the greater distributed, lower energy signals generated by the perfect bonds. It was attributed to the perfect bonds allowing steadier crack propagation, as opposed to the induced voids or disbond's creating possible slip-stick. Ducept *et al* [4], using a mixed-mode bending set-up with aluminium and glass/epoxy composites, have observed that cumulative AE signal amplitudes to be greater in the vicinity of failure initiation (due to elasticity) for adhesively bonded joints, which also agreed with conclusions made by other researchers. They also observed that the bonded DCB specimens created more AE signals after failure initiated and very little throughout the increased applied load, as with the 3-ENF specimens. Ohsawa *et al* [5] obtained similar conclusions for 4-ENF specimens using composite substrates, as discussed, with cumulative AE energy increasing towards specimen failure. Benmedakhene *et al* [6] used strain gauges into the apparatus to be considered for DCB testing methods in furthering the investigation of the strain-energy release rate. Although their study found correlations between loading rate and strain-energy release rate, they did not attempt to identify whether there was difference in AE sources occurring within the AE responses.

Although a great deal of research works are available in the literature regarding mechanical testing of adhesive bonded structures, there is still a limited work on using AE as a technique that may identify particular mechanical phenomena that may occur through adhesive failure. Therefore, the aim of this paper is to investigate employing AE for monitoring the failure onset of metal to metal and metal to composite plates and gain more insight into failure modes and in particular Mode I and II. AE may be integrated in order to obtain traits of different AE sources between the adhesive properties, varied bond quality and substrate material, through experimentation of failure Modes I and II.

2. Experimental procedures

2.1 Specimen manufacture

Carbon Fibre Composite sheets were created using a resin infusion method. This process involved six layers of pre-woven carbon fibre were cut into sections roughly 350 mm x 250 mm, this allowed for excess around the edges. The 2-part epoxy resin was drawn through the layers using a vacuum suction method. This setup was left for 1 week before the layers were cut into multiple specimens of 200 mm x 25.4 mm. The metallic substrates were manufactured using EN AW-6082/T2, 25.4 x 6.35 x 5000 mm aluminium alloy bar and was cut and milled to individual test specimen lengths.

The adhesive bonds between the substrates were achieved through a process of surface preparation, adhesive activation, adhesive application, and uniform force application between substrates. All of the substrates were then surface prepared through a process of sanding and acetone rinse removing any impurities before the adhesive application. Following the surface preparation, the application of the Loctite 7649 Activator was applied to the surface of the specimens and let to air dry. At this stage Dry PTFE Spray was used to act as a pre-crack, a length of 140 mm was covered so the remaining length was generously coated with the spray. Once dry, either the Loctite EA 3430 brittle or the AA 326 ductile adhesives were used to apply the 250 µ shims used to keep a consistent adhesive thickness. The adhesive was then applied generously, to ensure complete surface coverage. The specimens were then cured at an average temperature of 19.6 °C and humidity of 19.2 % for duration of a week.
Adhesive bond quality was investigated through three levels of control; 100%, 75% and 65% of the bonded surface area. Circuit boards were cut to the length of 200 mm and a width of 25.4 mm after the holes were drilled, as this coincides with the specimen length. Hole diameters for 3.15 mm were used for the 25% reduction and both 3.15 mm and 2.5 mm for the 35% surface area reduction. This allows a layer of PTFE spray to be applied through the holes onto surface of the specimen substrate.

2.2 Double cantilever beam (DCB)

The rig adaptor setup (see figure 1) can be inserted into the Instron 3382 tensile test machine to be pulled apart at a user-defined rate through the BlueHill 3 software. Strain rate was selected based on BS ISO 25217 [6], it was decided that this investigation would use 0.5 mm/min and 2 mm/min for metal-to-metal and metal-to-composite specimens, respectively.

Figure 1: DCB experimental set-up2.

2.3 End Notch Flexure (ENF)

The 3-ENF setup required the calculation of the bending moments to calculate the yield point of both of the combinations of metal and composite specimens (see equation 1). The calculation resulted in a total force of 2014 N before the metal-to-metal specimen yielded.

$$F = \frac{2\sigma_{max} b h^2}{3L} \quad (1)$$

Preceding the manufacture of the specimens, WaveMatrix Dynamic and Fatigue Materials Testing Software was used to program the Instron Model 1342 hydraulic machine for experimentation. The Instron Model 1342 has a maximum compressive or tensile load of

10 metric tons (100 kN), with a maximum crosshead movement of 50 mm in either direction (see figure 2). The rate at which the ram would be working was set up through the WaveMatrix software through two control methods for the different specimen combinations. It was decided that this investigation would use -0.5 mm/min and -2 mm/min for metal-to-metal and metalto-composite specimens, respectively, where the ramping rate value is negative due to ram moving in the upward direction towards the top roller.

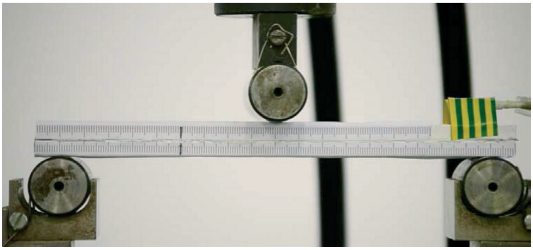

Figure 2: 3-ENF experimental set-up

2.4 Acoustic Emission

A Micro-80D differential AE sensor manufactured by Physical Acoustics Ltd was used throughout the investigation. The sensor has a useful frequency response over the region of 100 – 1000 kHz and features electrical isolation between the sensing element and the cavity in order to increase the sensors ability in applications featuring high background noise. The frequency at which the AE sensor most efficiently converts energy, the resonance frequency, was determined to be 340 kHz. Silicone grease was applied to the sensor before attaching to the specimen surface using electrical tape. The silicone grease was applied in order to improve the transmission of the AE signal between the specimen surface and the AE sensor; hence the imperfect connection caused by air gaps between the sensor and the specimens' microscopic surface roughness was minimised [7].
The AE sensor was connected to a pre-amplifier that was utilised to amplify the acquired signals gain and could be varied between 20, 40 and 60 dB. The pre-amplifier was connected to an in-house-built 4-channel signal conditioning unit (SCU) that was coupled with a gain programmer in order to supply 28V of power, coupled with adjustable gain control. The SCU transmits the adjusted signal to a National Instruments (NI) BNC-2120 shielded connector block in order to complete the systems signal transmission to the data acquisition card (DAQ). The signals were interpreted through a computer using a NI PCI-6115 DAQ in order to obtain the raw signal data and convert it to a binary file within the LabVIEW software for further analysis using Matlab.

2.5 Signal processing

An estimate of the distribution of a signal's energy across the frequency domain can be characterised using the power spectral density (PSD) method of quantifying the power contained in a signal at different frequencies. Welch's power spectral density estimate was utilised in order to convert the AE signal into the frequency domain from the time domain using spectrum estimation.
In order to achieve greater level of comparison between the frequency spectrums obtained in testing, a quantification method was devised. where the signals can be filtered between ranges of frequency in order to evaluate the spectral energy contained within those bands. These

frequency ranges are then quantified with a level of energy and can be compared as a proportion as seen in equations 2 and 3.

$$Total\ Energy = Energy\ of\ Range\ 1 + Energy\ of\ Range\ 2 + \cdots + Energy\ of\ Range\ n \quad (2)$$

$$\frac{Energy\ of\ Range\ n}{Total\ Energy} \times 100\% = Energy\ Proportion\ of\ Range\ n \quad (3)$$

A 5th order, low pass digital Chebyshev bandpass filter with 0.9 peak to peak ripple was utilised to filter the raw AE signal data for further analysis of the AE spectrums. The sensor had a useful frequency range of 100-1000 kHz therefore the signals acquired out-with this frequency range were assumed to be electrical noise. Different AE sources would require different parameters of gain, threshold, sampling frequency, number of scans and recording time in order to capture the signal accurately. The experimental parameters of the testing conducted through the investigation are established in table 1.

Table 1- Experimental settings for the mechanical testing of the specimens

SCU Gain (dB)	Pre-amp Gain (dB)	Threshold (V)	Sampling Frequency (MHz)	Number of Scans (datapoints)	Time/Signal Duration (s)
12	20	0.1	2.5	2500000	1

PLB tests were conducted upon each of the specimen combinations in order to understand the signal propagation through each of the different specimens. This allowed for a calibration to be set before continuing onto the two modes of failure. Systematic coding has been employed in order to allow an effective means of communicating individual specimen types and their representative data, where table 2 presents the coding system.

Table 2 - Specimen coding system

	Mode of Testing		Material		Adhesive Type		Bond Quality		
Type	DCB	3-ENF	Metal-Metal	Metal-Composite	AA 326	EA 3430	100%	75%	65%
Coding	DCB	3-ENF	MM	MC	D	B	100	75	65

3. Results and discussion

The loading output plots of both the ductile and brittle adhesives for the DCB experimentation were divided into three identified phases of mechanical significance (see figure 3a): initial pre-crack extension of the specimen (I), elastic region of the substrate and adhesive (II), and the adhesive de-bonding to the final adhesive failure (III). Throughout analysis of the 3-ENF testing loading graphs, it was clear that the graphs differ from the DCB experimentation. The difference in the elastic properties of the two adhesives resulted in differing loading traits for the mode II failure, especially regarding stage of adhesive failure (see figures 3b & 3c). The mode II loading graphs for the ductile specimen were divided into the following phases:

initial roller loading upon the specimen (I); elastic region of the substrates' and adhesive (II); yielding and failure of adhesive (III); and post-final adhesive failure (IV). It becomes apparent that the higher elasticity of the ductile adhesive resists adhesive failure and hence survives throughout the substrates' elastic region. The mode II loading graphs for the brittle specimen were divided into the following phases: initial roller loading upon the specimen (I); adhesive stressing and failure (II); elastic region of the substrates' (III); and the yielding of the specimen substrates' (IV). The brittle properties of the adhesive allow the in-plane shear failure to occur during the elastic stress region of the aluminium substrates.

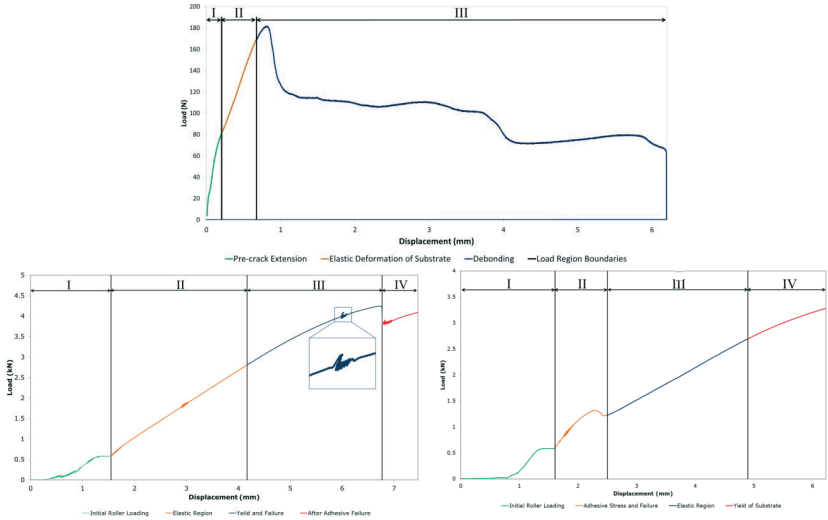

Figure 3: General loading phases for all specimen of: (a) DCB; (b) 3ENF.D, featuring magnified indication of specimen slippage; and (c) 3ENF.B

Analysis of the AE data produced from the DCB.MM.D.100 specimen showed an expected steady increase in AE energy towards adhesive failure, which was in-line with the findings of [5]. When filtered between 100-1000 kHz, the AE signal typically featured an increase in maximum AE amplitude along the time evolution (see figure 4). The energy in an AE signal is directly related to the AE amplitude; therefore, it can also be stated that the increase in AE amplitude was due to the AE source nearing the AE sensor. The AE source approached the sensor due to the adhesive failure occurring along the specimen length beginning from the opposing end where the sensor was located. This phenomenon was noticed throughout all DCB test specimens, although especially visible in regards to the DCB.MM.D.100 specimen.

Changes in the loading graph were deemed significant as they are seen to correlate to different mechanics of de-bonding, showing capability of the AE technique in regards to adhesive bonds. AE amplitudes of particular interest were designated for further AE analysis where typically, the first significant signals were generated within Phase III. These points were chosen due to their significant AE magnitude above the background noise and their relation to specific recognisable points on the loading graph that may be of mechanical significance. Where the loading enters Phase III, the adhesive accumulates stress, slowing the rate of loading and may produce an AE response; whereas reduction in loading identifies an adhesive failure. Adhesive

stressing and failure have been identified as different potential AE sources and allowed a more complete comparison to be discussed.

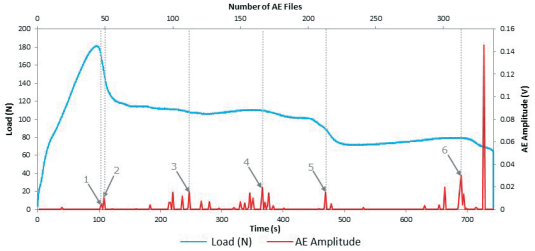

Figure 4: Specimen DCB.MM.D.100: load & AE amplitude vs. time

Similar to the double cantilever beam results, the loading graphs for each individual 3ENF test specimen were aligned with the corresponding maximum AE amplitudes. Initial AE analysis of the 3-ENF experiments proved to be less uniform throughout the differing combinations than that of the DCB, due to the mechanical properties of the adhesives with the particular mode of failure. Figure 5a shows the AE signals for the 3ENF.MM.D.100 specimen. The MM.D specimens showed no prominent AE signals in Phase I of the failure for all bond qualities, including the transition stage. The lack of AE signals in Phase I for the MM.D adhesive specimens was consistent with the analysis of the MC.D specimens.

However, there was a notable difference where there was a reduced duration of each phase. This analysis shows the applicability of the AE technique in regards to the mode II adhesive fracture failure; however, the ductile adhesive specimens cannot be concluded upon definitively in this instance due to plastic deformation of the substrate before adhesive failure. This would allow generalised conclusions to be made, however, distinction between the AE signals created by the ductile adhesive and the chosen substrates may be impossible for mode II experimentation.

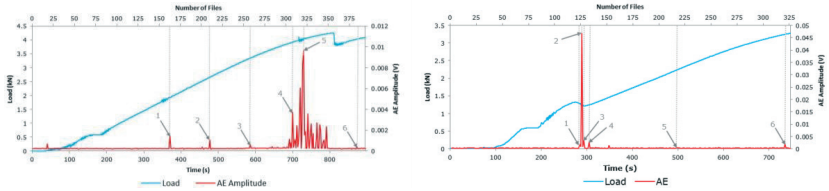

Figure 5: Load & AE amplitude vs. time for: (a) Specimen 3ENF.MM.D.100; and (b) Specimen 3ENF.MM.B.100

The differing load graph profile for brittle adhesives (see figure 5b) compares well with the generated AE signals in mode II experimentation as previously discussed for Mode I results. The 3ENF.MC.B results showed a single recognisable AE signal at the apparent failure of adhesive, where the loading graph justifies this event with a similarly short-sharp incident. Following the brittle adhesive failure, there were notable AE responses acquired in the elastic region of the substrate loading. The brittle failure may have resulted in frictional forces occurring between the substrates during further loading where the substrates attempt to move in shear. However, it has previously been discussed that AE responses in the elastic region of

the substrate and adhesive loading, may be due to the mechanical processes occurring during elastic deformation.

Certain specimens were found to fail out with the elastic region of the substrate and therefore, the adhesive failure may be convoluted within differing AE sources. A variety of the different potential AE sources have been identified for the 3-ENF experimentation in order to allow a valid, complete comparison to be discussed; these identified AE files and their respective sources were compiled in order to provide a valid comparison for discussion. In addition, there have been notable AE responses found at locations where the substrate is loading within the elastic and plastic regions therefore would require analysis in order to define the AE sources' response.

The frequency spectra of the experimentation AE signals featured a wider frequency range that spanned the entire useful range of the AE sensor. The spectral energy contained in the higher frequencies (i.e. greater than 400 kHz) were found to be very small in proportion to the areas of significance. Therefore, the divisions of the frequency ranges into three significant spectral energy contents (100-300, 300-400 and 400-700 kHz) were used in this study.

Proportioning the frequency content into percentages allowed normalisation of the data and hence provided a standard comparison. The effect of normalising the individual max amplitude AE events chosen for the six particular files of data which were identified in figure 4. Figure 6 shows spectral energy proportion for individual AE events. As can be seen, the low frequencies have dominant spectral energy content over the higher frequencies. A comparison between the selected AE data files of spectral energy proportion may highlight a potential correlation between the mechanical phenomena occurring and the location of energy content in the frequency spectrum. An exponential trend line was integrated to the plot in order to determine a correlation between the AE source and the progression of file number. The progression of the file number can also be related to the evolution of time and hence a variation in distance along the specimen length. It would be beneficial to acquire the AE responses during initial pre-analysis experimentation when there was no adhesive bonding incorporated in specimens. This would allow further analysis of the exact AE responses generated with fewer additional potential AE sources acquired in the absence of the adhesive bonding.

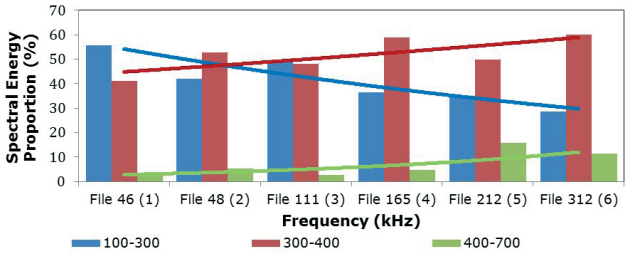

Figure 6: Spectral energy proportion for individual AE events chosen for DCB.MM.D.100 specimen (figure 4)

The early adhesive failure of the 3ENF.MM.B.100 specimens shown in figure 5b has allowed a more clear comparison of different AE sources. Potential AE sources of this particular specimen adhesive were identified to be either elastic or plastic substrate deformation. The chosen files 1-4 are all identified to contain an event within the adhesive failure location; whereas the files 5 and 6 were identified to contain an event within the elastic and plastic deformation regions of the substrates following the adhesive failure, respectively. Therefore,

it has been found that there was a difference in the frequency energy proportion dependant on the mechanical phenomena occurring and it may possible to differentiate between AE sources using this analysis method (see figure 7).

There was a noted difference in frequency spectra of particular mechanical phenomena that occurred through individual specimen experimentation, which was most recognisable through energy spectral proportioning analysis. It was determined that this was due to the change in frequency spectra along the length of the specimen with a stationary AE sensor and hence limited the comparisons that could be drawn as the AE source location shifted along the specimen length.

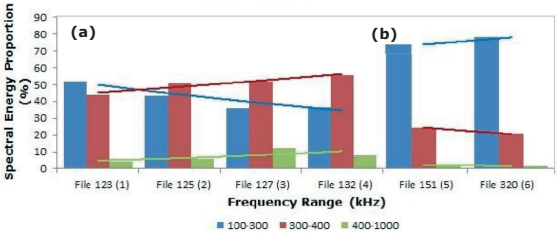

Figure 7: Comparison of the chosen AE files for 3ENF.MM.B.100 (figure 5b) with their respective spectral energy proportions showing two distinctive in AE sources: (a) adhesive failure; and (b) elastic/plastic substrate deformation

4. Conclusion

The aim of the investigation was to determine whether relationships exist for various adhesively bonded material combinations between the adhesive properties and the respective failure mode using their AE characteristics. The following is concluded:

- It was possible for the maximum AE amplitude method to select the AE events of mechanical significance (e.g. adhesive failure, substrate elastic deformation) for further identification through thorough analysis.
- It was possible to distinguish between the different AE sources of mechanical significance acquired from the selected AE maximum amplitude events (e.g. adhesive failure, substrate plastic deformation). However, it was proved difficult to propose a definitive AE trait for the mechanical phenomena occurring within specific AE event signals, for all adhesive types, bond qualities, and substrate configurations; therefore, all specimen combinations.
- There was a notable shift in spectral energy proportion as the AE source of mechanical significance (e.g. adhesive failure, adhesive stressing) varied along the specimen length for particular adhesive types, bond qualities, and substrate configurations; therefore, all specimen combinations. However, it was difficult to confirm this distinctive trait for all specimen combinations due to difficulty in confirming the location and exact mechanical source.
- The first significant maximum AE amplitude event for all adhesive types, bond qualities, and substrate combinations were relatable to the delamination tip (initiation of de-bonding).

- In general, AE energy and maximum amplitude was found to increase against displacement (and hence time evolution); where this was identified to be a result of the AE source approaching the AE sensor.
- AE identified the failure of the brittle adhesive in regards to the 3-ENF failure mode, with a cluster of significant maximum AE amplitudes occurring at adhesive failure; whereas the ductile adhesive's failures occurred in substrates' plastic region and therefore introduced another potential AE source.
- All DCB.MM.D specimens showed significant signs of delamination on the loading graphs with high elasticity whereas the DCB.MM.B specimens maintained a high, constant load before final failure.
- The DCB.MC tests also conformed to the three distinct phases, although Phase I and II occurred over a shorter period of time, which could be attributed to the adhesion properties of the CFRP, or the faster loading displacement rate.

References

1. BAK, K.M. et al., 2013. Study on the effect of adhesive thickness of single lap joints using acoustic emission and FEA. Insight-Non-Destructive Testing and Condition Monitoring, 55(1), pp. 35-41
2. LIM, A.S. et al., 2011. Damage sensing of adhesively-bonded hybrid composite/steel joints using carbon nanotubes. Composites Science and Technology, 71(9), pp. 11831189
3. NAYEB-HASHEMI, H. and ROSSETTOS, J. N., 1994. Nondestructive Evaluation of Adhesively Bonded Joints by Acousto-Ultrasonic Technique and Acoustic Emission. Journal of Acoustic Emission, 1994., pp 1-14.
4. DUCEPT, F., DAVIES, P. and GAMBY, D., 2000. Mixed mode failure criteria for a glass/epoxy composite and an adhesively bonded composite/composite joint. International Journal of Adhesion and Adhesives, 20(3), pp. 233-244
5. OHSAWA, I. et al., 2004. Development of a novel optical fiber sensor for AE detection in composites. Journal of Acoustic Emission, 21, pp. 176-186
6. BRITISH STANDARDS INSITUTION, 2009. BS ISO 25217:2009. Determination of the mode I adhesive fracture energy of structural adhesive joints using double cantilever beam and tapered-double cantilever beam specimens. London: British Standards Institution.
7. Droubi, M.G., Reuben, R.L. and White, G., Acoustic Emission monitoring of abrasive particle impacts on carbon steel. Proceedings IMechE, Part E, Journal of Process Mechanical Engineering, 226, (2011), 187-204.